Title

Enhanced genome integrity maintenance and few large stress-mitigating changes in *Arabidopsis halleri* extreme-habitat local adaptation

Authors

Gwonjin Lee[1], Julia Quintana[1], Hassan Ahmadi[1], Lara Syllwasschy[1], Justin E. Anderson[1], Björn Pietzenuk[1] and Ute Krämer[1, *]

Affiliations

[1]Molecular Genetics and Physiology of Plants, Ruhr University Bochum, Bochum Germany

***Corresponding author**

Professor Dr. Ute Krämer, Molecular Genetics and Physiology of Plants, Ruhr University Bochum, Universitaetsstr. 150 ND3/30 Box 44, D-44801 Bochum, Germany; **Email**: Ute.Kraemer@ruhr-uni-bochum.de

ORCID: 0000-0003-2207-3975 (GL), 0000-0002-5145-3590 (JQ), 0000-0001-9354-6886 (HA), 0000-0002-5388-3578 (LS), 0000-0001-7642-4641 (JEA), 0000-0002-2688-3783 (BP), 0000-0001-7870-4508 (UK)

Classification: Biological Sciences (major), Plant Biology (minor), (Evolution, Ecology)

Keywords: Evolutionary adaptation, intra-species trait variation, anthropogenic environmental change, heavy metal, tolerance, metal hyperaccumulation, Brassicaceae, Arabidopsis-related model systems

Author Contributions: Designed research: UK, GL, JQ, JEA, BP; conducted experiments: GL, JQ, HA, LS; analyzed data: GL, UK, JQ, HA, BP, LS; wrote paper: GL, UK, with contributions from JQ, HA, BP.

Abstract

Heavy metal-rich toxic soils and ordinary soils are both natural habitats of *Arabidopsis halleri*, different from closely related plant species including *A. thaliana*. Here we demonstrate enhanced Cd hypertolerance and attenuated Cd accumulation in plants originating from the most highly heavy metal-contaminated *A. halleri* site in Europe at Ponte Nossa (Noss/IT), compared to *A. halleri* from non-metalliferous (NM) sites at a small and a larger phylogenetic distance. In the two populations from NM sites, hundreds of Cd-responsive transcripts mostly reflect the activation of Fe deficiency responses, whereas no single transcript showed differential abundance between Cd-exposed and untreated control plants from the metalliferous (M) site Noss. Among thousands of transcripts exhibiting between-population differential abundance in vegetative stage tissues, meiotic cell cycle functions were overrepresented, with an activation in plants from Noss. Between-population differences in transcript levels were highest for *ARGONAUTE 9* (*AGO9*) and the synaptonemal complex transverse filament protein-encoding genes *ZYP1a/b*, which are pre-meiosis- and meiosis-specifically expressed, respectively, in *A. thaliana*. Moreover, transcript levels of *IRON-REGULATED TRANSPORTER 1* (*IRT1*) were much lower in Noss and those of *HEAVY METAL ATPASE 2* (*HMA2*) were far higher compared to both Pais and Wall, largely explaining between-population differences in Cd handling. Immunoblots for ZYP1 and IRT1 validated our observations at the protein level. In summary, plant adaptation to extreme abiotic stress is associated with globally enhanced somatic genome integrity maintenance including previously unsuspected gene functions, as well as a small number of constitutive alterations in stress-related functional networks.

Significance Statement

The re-establishment of ecosystems in extreme environments, which often arise through rapid anthropogenic change, relies on rare plants capable of colonizing such bare sites. As sessile organisms, these plants must possess effective physiological adaptations for coping with extraordinary abiotic stress levels, but the underlying molecular basis remains unknown. Here we examine intra-species transcriptomic divergence associated with an extreme-stress habitat, soil containing toxic levels of heavy metals, in somatic tissues of *Arabidopsis halleri*: Among activated biological processes, functions of the *A. thaliana* meiotic cell cycle are the most prominent, and we argue for their partly uncharacterized roles in genome integrity maintenance. Additionally, few but drastic differences in metal homeostasis gene expression largely explain environment-specific metal handling in different *A. halleri* populations.

Introduction

Heavy metals, such as zinc (Zn), cadmium (Cd) and lead (Pb), are naturally omnipresent in the biosphere at very low levels. Their concentrations can be regionally elevated and are on rare sites extremely high locally, as a result of geological anomalies. Human activities, for example ore mining, metallurgical processing and sewage sludge deposition, contribute to anthropogenic contamination of the biosphere with heavy metals, threatening environmental and human health (1, 2). Heavy metal-enriched habitats often host characteristic ecological communities, especially where human activities have introduced extremely high, toxic levels of heavy metals only recently after the beginning of the industrial revolution (3). Here we use comparative transcriptomics to uncover the molecular basis of local adaptation to a highly heavy metal-contaminated soil in a land plant as a complex multi-cellular eukaryotic organism.

The Brassicaceae species *Arabidopsis halleri* in the sister clade of the genetic model plant *Arabidopsis thaliana* has repeatedly colonized highly heavy metal-contaminated, so-called metalliferous (M) soils (4). Natural populations of *A. halleri* are also found on non-contaminated (non-metalliferous, NM) soils. Irrespective its habitat soil type, *A. halleri* is as a Zn and Cd hyperaccumulator species (3, 4). The about 750 known hyperaccumulator plant species are land plants, of which at least one individual was identified to accumulate a metal or metalloid in its above-ground tissues to concentrations more than one order of magnitude above critical toxicity thresholds of ordinary plants, at its natural site of growth in the field (5). Hyperaccumulation in plants can act as an elemental defense against biotic stress, and the associated species-wide heavy metal tolerance can facilitate the colonization of M soils by *A. halleri* (6).

Cross-species comparative transcriptomics studies of *A. halleri* and *A. thaliana* established tens of candidate metal homeostasis genes for roles in metal hyperaccumulation or metal hypertolerance, which encode various transmembrane transporters of metal cations and isoforms of a metal chelator biosynthetic enzyme (7-9). Subsequent work demonstrated functions in metal hyperaccumulation or hypertolerance for some of these genes. The key locus making the largest known contribution to both metal hyperaccumulation and hypertolerance in *A. halleri* is *Heavy Metal ATPase 4* (*HMA4*), which encodes a plasma membrane P_{1B}-type metal ATPase mediating cellular export for xylem loading of Zn and Cd in the root (8, 10). Transcript levels of *HMA4* are substantially higher in *A. halleri* than in *A. thaliana* independently of cultivation conditions, as observed for many candidate genes. A combination of modified *cis*-regulation and gene copy number expansion accounts for high expression of *HMA4* (10). Other candidate genes with experimentally demonstrated functions in *A. halleri*

include *NAS2* (11) contributing to Zn hyperaccumulation, *MTP1* (encoding a vacuolar Zn^{2+}/H^{+} exchanger) acting in Zn tolerance (12) and *CAX1* (Ca^{2+}/H^{+} exchanger 1) functioning to enhance Cd tolerance (13). While metal hyperaccumulation and hypertolerance are species-wide traits in *A. halleri*, there is additionally a large extent of within-species variation in the levels of metal accumulation, metal tolerance and gene expression (4, 14-16).

Within-species transcriptomic differences between *A. halleri* populations originating from M and NM soils can provide insights into the molecular alterations associated with the natural colonization of M soils, but they have remained unexplored thus far. To address local adaptation to M soil in *A. halleri*, we focused here on the population at the most highly heavy metal-contaminated *A. halleri* site in Europe at Ponte Nossa (Noss/IT) according to a large field survey (4). Noss individuals were more Cd-tolerant and accumulated lower levels of Cd than both closely related *A. halleri* from a population on NM soil in the vicinity, Paisco Loveno (Pais), and more distantly related *A. halleri* Wallenfels (Wall), on NM soil in Germany. Further contrasting with plants of NM soil origin, transcriptomic Cd responses including the activation of Fe deficiency responses were attenuated in the highly Cd-tolerant population. Instead, a large number of transcripts differed in abundance in Noss (M soil origin) from both Pais and Wall plants (NM soil origins) irrespective of cultivation conditions. Differences comprised primarily the global activation of meiosis- and genome integrity maintenance-related functions in somatic tissues of Noss, accompanied by pronouncedly altered levels of few metal homeostasis transcripts known for central roles in Cd accumulation and basal Cd tolerance of *A. thaliana*. We confirmed exemplary differences at the protein level using immunoblots. Our results suggest somatic functions in *A. halleri* (Noss) for several known meiosis genes. This work provides insights into how land plants cope with rapid anthropogenic environmental change and extreme abiotic stress levels.

Results

Choice of populations and comparative physiological characterization

In a field survey of 165 *Arabidopsis halleri* sites across Europe, average soil Cd concentrations were highest at Ponte Nossa/IT (Noss) in both the total and hydrochloric acid-extractable soil fractions (900 and 203 mg Cd kg^{-1} soil, respectively; second highest at 130 and 87 mg Cd kg^{-1} soil, respectively)(4). Therefore, we chose the *A. halleri* population at this M site as the focal population in this comparative study, in combination with two populations at NM sites for comparison, one near Paisco Loveno (Pais/IT) approximately 38 km northeast of Noss, and one near Wallenfels (Wall/DE) about 520 km

to the North. Average soil total Cd concentrations in close proximity of the *A. halleri* individuals studied here were 700-fold higher at Noss than at Pais (Table S1).

In order to test for local adaptation of the Noss population to high soil Cd levels, we quantified Cd tolerance of individuals collected at each of the three sites in hydroponic culture in a growth chamber. Based on the proportion of individuals maintaining root growth in a sequential exposure test with stepwise increasing Cd concentrations, Noss was the most tolerant (Fig. 1a). Mean EC_{100}, the effective Cd concentration causing 100% root growth inhibition, was significantly higher for Noss (344 ± 98 μM Cd) than for Pais (219 ± 66 μM Cd) and Wall (221 ± 56 μM Cd) (Fig. 1b, Table S2).

In natural populations in the field, Cd concentrations accumulated in leaves of *A. halleri* at Noss were at least 20-fold higher than at Pais and 3-fold higher than at Wall (Table S1)(4). By contrast, Zn concentrations in leaves of field-collected individuals were similar in all three populations, despite vastly differing soil Zn levels. The leaf:soil ratio of Cd concentrations (Cd accumulation efficiency) in the field was highest in the Wall population from north of the Alps, suggesting attenuated leaf Cd accumulation at Noss compared to both Pais and Wall (Fig. 1c), in agreement with known general differences between M and NM *A. halleri* sites (4). Upon exposure to a sub-toxic concentration of 2 μM $CdSO_4$ in hydroponic culture for 16 d, Cd concentrations in roots of Noss (140 ± 74 μg Cd g^{-1} DW) were only 43% and 40% of those in Pais and Wall, respectively (Fig. 1d, Table S3). Leaf Cd concentrations were also lower in Noss (160 ± 74 μg Cd g^{-1} DW) than in Wall (about 52% of Wall; $P < 0.05$), and at about 76% of those in Pais. We additionally observed between-population differences in the accumulation of other nutrients (Fig. S1). Upon Cd exposure, Cu concentrations were higher, and Mn concentrations were lower than under control conditions in roots of Pais and Wall, but not of Noss (Fig. S1a and d). Fe concentrations were higher in roots of Noss and increased further under exposure to Cd, in contrast to the two populations from NM soils (Fig. S1e). In shoots of Noss, Fe concentrations were about twice as high (*ca*. 75 μg Fe g^{-1} DW) than in the shoots of the other two populations under both control and Cd exposure conditions (Fig. 1e). Taken together, these results showed that the Noss population of *A. halleri* is more tolerant to Cd than both Pais and Wall, supporting adaptation to local soil. This was associated with attenuated Cd accumulation and a distinct profile of tissue concentrations of micronutrient metals in Noss under standardized growth conditions in hydroponic culture.

Comparative transcriptomics

Transcriptome sequencing was carried out for a total of 72 samples, with three independent repeats of each experiment comprising root and shoot tissues of two genotypes from each of the three populations grown in control and Cd-amended medium for 16 d (0 and 2 µM $CdSO_4$; Table S4, Dataset S1). Principal component analysis (PCA) suggested predominant differences between root and shoot transcriptomes (Fig. S2a). In both roots and shoots, transcriptomes of the geographically neighboring populations Noss and Pais grouped closer together in the first principal component by comparison to the geographically distant Wall population (Fig. S2b, c).

Upon long-term exposure to a low level of Cd as applied here, transcriptomic differences compared to controls comprised a few hundred genes in both the Pais and Wall populations originating from NM sites (Fig. 2a and b, Fig. S3, Fig. S4). By contrast, in the more Cd-tolerant population Noss, no single transcript responded in abundance to Cd exposure under these conditions in either roots or shoots. To identify candidate transcripts that may contribute to the ability of the Noss population to persist on extremely highly heavy metal-contaminated soil, we thus examined the genes showing differential expression between populations (Fig. 2c and d, Dataset S2). As an initial set of candidate genes, we focused on those transcripts showing differential abundance between Noss (M) and both of the populations from NM soils, Pais and Wall. This identified 1,617 genes (801/599/217, higher in Noss/ lower in Noss / intermediate in Noss) in roots and 1,638 genes (797/604/237) in shoots under control conditions (under Cd exposure 848/697/236 and 1140/707/339 in roots and shoots, respectively) (surrounded by a red line in Fig. 2c and d).

Candidate genes differentially expressed in Noss

We subjected the genes expressed either at higher or lower levels in Noss compared to both Pais and Wall (DEGs; 0 µM Cd; Dataset S3) to a gene ontology (GO) term enrichment analysis (Dataset S4). Meiotic cell cycle (GO:0051321) was enriched in the group of more highly expressed genes in both root and shoot of Noss (Fig. 3a, b, Table S5). Among the genes within the GO term meiotic cell cycle, transcript levels of *ARGONAUTE 9* (*AGO9*) were substantially higher in both root and shoot tissues of the Noss in comparison to both the Pais and Wall populations (Fig. 3c, d, Table S6; Log_2FC = 6.6 and 4.4 to 4.6 in root and shoot, respectively; see Dataset S2). By contrast, present knowledge suggests that the expression of *AGO9* in *A. thaliana* is restricted to only a few cells during the early stages of meiotic megaspore formation (17, 18). Amino acid sequence alignment of AGO proteins in *A. halleri* and *A. thaliana* (Fig. S5) confirmed that *Ah*AGO9 is the closest *A. halleri* homologue of *At*AGO9 in

clade 3 of ARGONAUTE proteins (AGO4, -6, -8 and -9)(19). Sequence read coverage for *AGO9* obtained from gDNA of Noss and Pais suggested that *AGO9* is a single-copy gene (Table S7).

In the ontology class meiotic cell cycle, transcript levels of the two gene copies of *ZIPper I* (*ZYP1a* and *ZYP1b*) were also substantially higher in Noss than in both Pais and Wall (Fig. 3e-f, Tables S5 and S6). In agreement with this, immunoblot detection using an antibody directed against *At*ZYP1 suggested that leaves of Noss contain higher levels of ZYP1 protein than leaves of Pais (Fig. S6). Amino acid sequences of *At*ZYP1a and b are highly similar and conserved in *Ah*ZYP1a and b (Fig. S7). An additional 15 genes in roots and 10 genes in shoots of the GO meiotic cell cycle showed mildly elevated transcript levels in Noss compared to both populations of NM soil (see Fig. 3a and b, Dataset S4). The partly overlapping categories homologous recombination (GO:0035825), reciprocal meiotic recombination (GO:0007131), meiosis I cell cycle process (GO:0061982) and condensed chromosome (GO:0000793) were also enriched among transcripts of increased abundance in roots of Noss. Among 23 genes over-represented in GO terms associated with meiotic cell cycle and homologous/meiotic recombination, homologs of eight genes were reported to have roles in somatic DNA repair in *A. thaliana* (Table S5). Furthermore, sulfur compound metabolic process (GO:0006790), glucosinolate biosynthetic process (GO:0019761) and plastid (GO:0009536) were enriched among transcripts of decreased abundance in shoot tissues of Noss (see Dataset S4).

Differential abundance of metal homeostasis-related transcripts between populations

Next, we sought to identify metal homeostasis candidate genes contributing to the observed differences in Cd tolerance and accumulation between Noss and the two other populations. For this purpose, we intersected a manually curated list of metal homeostasis genes with the list of candidate transcripts (see Fig. 2e-g, $|\mathrm{Log_2FC}| > 1$, mean normalized counts across all samples > 2; Dataset S3, Table S8). Transcript levels of *Heavy Metal ATPase 2* (*HMA2*) and two *ZRT/IRT-like Protein* genes, *ZIP2* and *ZIP6*, were higher in roots of Noss than Pais and Wall (Fig. 3e). Root transcript levels of *Iron-Regulated Transporter 1* (*IRT1*), *Plant Cadmium Resistance 9* (*PCR9*) and *ZIP10* were lower in Noss (Fig. 3f). In shoots of Noss, transcript levels of *PCR8*, *HMA2* and *Cation/H*$^+$ *Exchanger 2* (*CHX2*) were higher than in both Pais and Wall (Fig. 3g).

The IRT1 transmembrane transport protein is known as the high-affinity root iron (Fe^{2+}) uptake system of dicotyledonous plants as well as the predominating path for inadvertent uptake of Cd^{2+} in Arabidopsis (20). Compared to Pais and Wall, an 84% to 92% lower expression of *IRT1* in Noss (see Fig. 3f) would provide an intuitive adaptive route towards plant Cd tolerance *via* exclusion (see Fig.

1d, Fig. S8). In *A. thaliana*, *IRT1* expression is under complex regulation at both the transcriptional and post-transcriptional levels (21). To test whether reduced IRT1 protein levels accompany low *IRT1* transcript abundance in Noss, we carried out immunoblot detection using an anti-*At*IRT1 antibody in subsamples of root tissues from plants cultivated under control conditions. At the size corresponding to IRT1 of Fe-deficient *A. thaliana*, we observed bands in both Pais and Wall, but IRT1 protein levels were below the limits of detection in Noss. Instead, we observed weak signals at higher apparent molecular masses corresponding to expectations for the mono- and di-ubiquitinated forms of IRT1, respectively (Fig. 3h)(22). In *A. thaliana*, the ubiquitination of IRT1 leads to its deactivation by removal from the plasma membrane through endocytosis (23). Sequencing-based transcriptomic data were validated by reverse-transcription quantitative real-time PCR (RT-qPCR; Table S9, Fig. S9).

Cd exposure elicits transcriptional Fe deficiency responses in both populations from NM sites

Upon exposure to Cd, we found different transcript abundance for 210 genes (upregulated 53, downregulated 157) in shoots and of 428 genes (upregulated 143, downregulated, 285) in roots of Pais. A similar number of 197 (upregulated, 65; downregulated, 132) in roots and 243 (upregulated, 98; downregulated, 145) in shoots responded to Cd in Wall (see Fig. 2a and b, Dataset S5). Of these, the responses of 44 genes in roots and of 84 genes in shoots were shared between both populations from NM soil, a larger number than expected by chance ($P < 10^{-50}$, hypoergeometric test). Transcriptomic Cd responses of both Pais and Wall were enriched in Fe deficiency responses (Fig. 4, Dataset S6). The associated enriched GO categories included cellular response to iron ion starvation (GO:0010106) among the upregulated transcripts, as well as intracellular sequestering of iron ion (GO:0006880) and ferroxidase activity (GO:0004322) among the downregulated transcripts in both roots and shoots.

Among transcripts known to increase in abundance in *A. thaliana* under iron deficiency, transcript levels of *Popeye* (*PYE*), *Basic Helix-Loop-Helix 38/39/100/101* (*bHLH38/39/100/101*) transcription factors, *Brutus* (*BTS*) and *Brutus-like 1* (*BTSL1*), as well as *Ferric Reduction Oxidases* (*FRO1* and *FRO3*), *Nicotianamine Synthase 4* (*NAS4*), *Zinc Induced Facilitator 1* (*ZIF1*), *Oligopeptide Transporter 3* (*OPT3*) and *Natural Resistance-Associated Macrophage Protein 3* (*NRAMP3*) increased under Cd exposure (Table S10a). A number of transcripts have roles in iron storage/sequestration, and their levels are downregulated under iron deficiency in *A. thaliana*. Of these, *Ferritin* (*FER1*, *FER3* and *FER4*) and *Vacuolar iron Transporter-Like protein* (*VTL1* and *VTL5*) transcript levels were downregulated in Cd-exposed Pais and Wall plants (Table S10b).

Further GOs enriched among transcripts downregulated in abundance in response to Cd were response to reactive oxygen species (GO:0000302), photosynthesis (GO:0015979), chloroplast thylakoid membrane (GO:0009535). The gene content of these, however, is less compelling in implicating the respective biological processes (see Table S10b; Datasets S5 and S6). Chloroplast thylakoid membrane is a child term of plastid (GO:0009536), which was enriched among transcripts present at lower levels in Noss than in both Pais and Wall. Six genes were in common between these (Table S11), of which one, *Light Harvesting Complex of photosystem II* (*LHCB4.2*), appears to function directly in photosynthesis. A more extensive search for transcripts that are Cd-responsive in both Pais and Wall as well as differentially expressed in the Noss population identified *Bifunctional inhibitor/lipid-transfer protein/seed storage 2S albumin superfamily protein* in the root and *NAD(P)-binding Rossmann-fold superfamily protein* in the shoot (Table S12). Finally, metal homeostasis protein-encoding transcripts upregulated in abundance upon Cd exposure in Pais or Wall were generally less abundant in Noss regardless of Cd treatment (Fig. S10, cluster R5 and S5). Conversely, metal homeostasis protein-coding transcripts that were decreased in abundance under Cd exposure in Pais or Wall were generally present at higher levels in Noss (Fig. S10, cluster R2 and S2). These between-population differences primarily comprised genes associated with Fe deficiency responses of *A. thaliana* as described above (see Fig. 4, Table S10), thus indicating against a constitutive proactive activation in Noss of the transcriptional Cd responses observed here in the Pais and Wall populations.

Elevated *AGO9* expression and lower transcript levels of long terminal repeat retrotransposons in Noss

Comparative transcriptomics suggested that in particular, *AGO9* transcript levels were higher in Noss compared to both Pais and Wall (see Fig. 3c and d). If this were indeed the case, then we would expect that long terminal repeat retrotransposons (LTR-TEs), target loci known to be transcriptionally silenced dependent on *AGO9* in *A. thaliana*, are less transcriptionally active in *A. halleri* from Noss than *A. halleri* from Pais and Wall (17). In Noss, transcript levels derived from LTR-TEs were lower in shoot tissues by comparison to both Pais and Wall and also lower in root tissues than in Pais (Fig. 5, Fig. S11, Dataset S7).

Discussion

Divergent transcript levels between populations arise more abundantly than divergent transcriptomic responses to Cd

To identify the molecular alterations associated with plant adaptation to extreme abiotic stress, we conducted comparative transcriptomics of *A. halleri* populations from contrasting environments of origin across both a small and a larger phylogenetic distance (see Fig. S2 and S11). In line with their origin from the most highly Cd-contaminated *A. halleri* site known in Europe, our data supported environment-dependent phenotypic differentiation in *A. halleri* and adaptation to high soil Cd levels at Noss (Fig. 1). Transcript levels of a few hundred genes differed between Cd-exposed and unexposed *A. halleri* plants from the two populations originating from NM soils, Pais and Wall. Thus, these plants attained a different transcriptomic state in the presence of Cd through a process that must involve the initial interaction of Cd^{2+} with primary Cd-sensing or -sensitive sites, of which the molecular identities are yet unknown. By contrast, in *A. halleri* from the Noss (M) population, there was no single gene of which transcript levels differed between the 2-µM $CdSO_4$ and the control treatment (Fig. 2). This implies that in Noss, Cd^{2+} was either effectively kept away from all Cd-sensing and -sensitive sites, or Cd^{2+} did not result in any transcriptomic adjustment within a timeframe relevant for our harvest after 16 d of exposure. Given that Noss is more Cd-tolerant than both Pais and Wall (see Fig. 1), the molecular mechanisms conferring tolerance must then either be active also in the absence of Cd, or alternatively their implementation operates downstream of transcript levels, for example at the translational or post-translational level.

Several thousand transcripts differed in abundance between the Noss (M) population of *A. halleri* and either one of the two populations originating from NM sites irrespective of Cd exposure (Fig. 2; see also Fig. S10). This suggests that between-population transcriptomic divergence is substantial even among geographically proximal and phylogenetically closely related *A. halleri* populations Noss and Pais, by comparison to between-population differences in responses to Cd exposure. Similarly, cross-species comparative transcriptomics studies identified responses to metal exposure in *A. thaliana*, a species with only basal metal tolerance, whereas there were no remarkable additional species-specific responses among metal homeostasis genes in the metal-hypertolerant species *A. halleri* (8, 24). Instead, tens of genes with predicted roles in metal homeostasis were more highly expressed in *A. halleri* compared to *A. thaliana* irrespective of the growth conditions.

Constitutive activation of meiosis-related genes and large alterations in few metal homeostasis functions in *A. halleri* from Noss

Meiosis is essential for sexual reproduction in eukaryotes and consists of a series of two consecutive cell divisions generating four haploid daughter cells that are genetically unequal among one another and compared to the mother cell (25). Recombination takes place during the first meiotic cell division (meiosis I) through the formation of DNA double-strand breaks followed by homologous recombination between homologous chromosomes paired in the synaptonemal complex. In seed plants, meiosis occurs exclusively in male and female gametophyte precursor cells during the reproductive phase of the life cycle. Yet, the gene ontology "meiotic cell cycle" was overrepresented among transcripts of higher abundance in somatic tissues of Noss by comparison to both Pais and Wall (Fig. 3, Table S5, Dataset S4). This included genes functioning during entry into meiosis (*AGO9*, *SWI1*), cohesion complex (*SMC3*), synaptonemal complex (*ZYP1a/b*), recombination and its control (*PRD3*, *BRCA2B*, *MHF2*, *MSH5*, *FLIP*), for example (25). In addition to its role during meiosis, DNA double-strand break repair (DSBR) through homologous recombination (HR) functions to maintain genome integrity following DNA damage in somatic cells (26). Exposure of plants to an excess of aluminum, boron or heavy metal ions can cause DNA damage (27-30). Of the meiosis-related genes identified here, there is evidence for an additional involvement in somatic HR-mediated DSBR for *BRCA2* (31), *EME1A/B* (32), *HEB2* (30), *FLIP* (33, 34), *RPA2B* (35) and *ERCC1* (36) in *A. thaliana* (Table S5; Dataset S4). *ERCC1* was additionally implicated in non-HR nucleotide excision repair (37).

The two most strongly differentially expressed meiosis-related genes, *AGO9* and *ZYP1a/b*, are thought to function exclusively in reproductive development of *A. thaliana*. *AGO9* is required pre-meiotically to prevent the formation of excessive gametophytic precursor cells in *A. thaliana* (18). It is expressed in a single layer of somatic companion cells surrounding the megaspore mother cell, as well as in pollen. *At*AGO9 was proposed to act in the silencing of pericentromeric TEs, predominantly long terminal repeat retrotransposons (LTR-TEs), in the ovule through the interaction with 24-nucleotide small RNAs (17). Like other organisms, plants generally inactivate TEs in order to maintain genomic stability. Exposure to abiotic stress, including also heavy metal exposure, can result in the expression and transposition of some TEs, especially LTR-TEs, in plants (38) and other organisms (39). It is possible that the elevated expression of *AGO9* in somatic cells of *A. halleri* from Noss counteracts LTR-TE activation as an adaptation to their high-stress natural environment of origin. In agreement with this hypothesis, transcripts derived from LTR-TEs were present at overall lower levels in both

root and shoot tissues of Noss compared to Pais (Fig. 5). We detected no increase in the levels of transcripts derived from LTR-TEs or any other TEs at 2 µM Cd compared to control conditions. It is possible that an increase in TE expression occurs at different times after the onset of Cd exposure, at higher levels of Cd exposure which plants are likely to encounter at the Noss site at least temporarily (40), or in response to other abiotic stresses or combined stress exposure, in nature (Table S1). Published circumstantial evidence implicated *AGO9* also in DNA damage repair in seedlings of *A. thaliana* (41). Future work will be required to understand the biological functions of *AGO9* in somatic tissues of *A. halleri* and *A. thaliana*.

ZYP1a/b in *A. thaliana* is a tandem locus of two highly similar genes positioned head-to-head, which encode the transverse filament protein of the synaptonemal complex, a structure that mediates the pairing of homologous chromosomes for recombination during meiosis I (42). Loss-of-function of *ZYP1a/b* increases the number of non-homologous meiotic recombination events in *A. thaliana* (43). Here we observed enhanced expression of *ZYP1* in somatic tissues of *A. halleri* from Noss at both the transcript and protein levels (Fig. 3; Fig. S6), consistent with a biological function of this protein in somatic cells of above-ground tissues that remains to be analyzed in the future.

We propose that our results reflect a constitutive activation of genome integrity maintenance as a component of extreme abiotic stress adaptation of *A. halleri* at Noss. The genes newly implicated here in somatic genome integrity maintenance may have remained unidentified in the past because their functions are specific to *A. halleri* or because very low expression levels may be sufficient in *A. thaliana*. Cd is not the only abiotic stress factor at the Noss site in the field. Soil adjacent to the roots of *A. halleri* plants at Noss contained maximum levels also of Zn, total and extractable Pb (32,900 and 7,010 µg g^{-1}, respectively) and Cu (7,110 and 1,630 µg g^{-1}, respectively) out of 165 European sites hosting natural populations of *A. halleri* (Pais/NM: see Table S1, 73.1 and 4.93 µg Pb g^{-1} soil as well as 22.5 and 0.757 µg Cu g^{-1} soil, total and extractable, respectively)(4). Moreover, Noss is located at the southern edge of the distribution range of *A. halleri*, which may render light/UV, drought or high temperature stress, known to prevail on bare M sites, even more relevant abiotic environmental factors (44).

Attenuated Cd accumulation in *A. halleri* from Noss (see Fig. 1) observed here in hydroponics is consistent with earlier results from the cultivation of Noss and Wall on an artificially Cd-contaminated soil (4) and with results obtained in hydroponic culture on accessions collected nearby (14, 15). Among metal homeostasis genes, we observed substantially reduced *IRT1* expression in roots of Noss

compared to both Pais and Wall at both the transcript (Fig. 3f) and protein level of the transport-active form (Fig. 3h). This can account for both enhanced Cd hypertolerance and attenuated Cd accumulation in *A. halleri* from Noss when extrapolating from *A. thaliana irt1* mutants (20). Taking our data together, comparably high levels of iron (Fig. S1) in Noss plants appear to arise independently of IRT1 (Fig. 3h), which warrants further study.

Distinctly higher transcript levels of *HMA2* in both roots and shoots of Noss (Fig. 3e, g) when compared to both the Pais and the Wall populations suggest that enhanced cellular export of Cd contributes to enhanced Cd hypertolerance in this population. Alongside HMA4, the plasma membrane efflux pump HMA2 mediates root-to-shoot translocation of Zn in *A. thaliana* and can also transport chemically similar Cd^{2+} ions (45). *HMA2* transcript levels are present in roots of Zn-deficient *A. thaliana*, in particular (46). To further address a possible role of *HMA2* in the adaptation of *A. halleri* to local soil composition, localization of the cell types expressing *HMA2*, as well as genetic approaches, will be required.

Cd exposure induces Fe deficiency responses in both populations from NM sites

In the Wall and Pais populations from NM soils, we observed Fe deficiency response-like transcriptomic changes upon exposure to 2 µM Cd for 16 d (Fig. 4; Table S10). Plants that are non-hypertolerant to metals activate aspects of Fe deficiency responses when exposed to an excess of heavy metals, for example Cd (47). Consequently, our observation may be seen as unsurprising. However, previously published results in *A. thaliana* were from heavy metal treatment conditions causing a mix of toxicity symptoms and acclimatization responses. By contrast, in this present study the Cd treatment condition was far below toxicity thresholds of *A. halleri* that is known for species-wide Cd hypertolerance (Fig. 1). Our data suggest that even under exposure to very low sub-toxic Cd concentrations, transcriptional responses of *A. halleri* reflect symptoms of nutrient imbalances caused by Cd and must have a compensatory role in acclimatization at the same time.

Transcriptomics studies reported Fe deficiency responses in *A. halleri* from the PL22 (M) population, but not in the I16 (M) population from close to Noss (M), in response to high-Zn exposure (16). Moreover, a highly Cd-hyperaccumulating accession of *Noccaea caerulescens* exhibited a Cd-induced Fe deficiency response, by contrast to a low Cd-accumulating accession (48). Both of these earlier studies were lacking the comparison with a population from an NM soil environment, in

contrast to the work presented here. Unsurprisingly, central aspects of the identified metal responses relating to Fe acquisition systems and tissue Fe contents are different here (Fig. S1, Table S10).

The conserved steady-state hypothesis (40) postulates that plant adaptation to high soil Cd entails both attenuated cellular Cd uptake and the balancing of elevated rates of inadvertent Cd influx through constitutively elevated rates of sequestration away from internal cellular Cd-sensing/-sensitive sites. This present work implicates alterations in the expression of *IRT1* and *HMA2*, respectively, in these two processes, for example. The conserved steady-state hypothesis also postulates that these processes operate constitutively in plants at rates adjusted to the local Cd levels in the soil of origin to maintain internal cellular Cd at identical levels in contrasting natural habitats. This could explain the transcriptional responses to Cd-induced nutrient imbalance in Pais and Wall, and their absence in Noss in this study. In an extreme environment, quantitatively larger spatial and temporal variation in the respective stress factor requires enhanced capabilities for the protection from and repair of cellular damage, as was postulated (40). Our study implicates genome integrity maintenance by LTR-TE silencing and DSBR in plant adaptation to extreme stress, with contributions of hitherto unsuspected gene functions. In summary, our results provide a systems account of plant evolutionary adaptation to an extreme environment, highly heavy metal-contaminated soil, following rapid anthropogenic environmental change.

Materials and methods

Plant material and growth conditions

Cuttings were made of *A. halleri* ssp. *halleri* O'Kane & Al-Shehbaz individuals originating from the field (4) and pre-cultivated hydroponically for 4 weeks to obtain vegetative clones. Experiments were conducted in 1x modified Hoagland's solution (7) with weekly exchange of solutions. In Cd tolerance assays, plants were sequentially exposed to step-wise increasing concentrations of $CdSO_4$ (0, 25, 50, 75, 100, 125, 150, 175, 200, 250, 300, 350, 400 and 450 µM) once per week in a growth chamber (10-h light at 90 µmol photons m^{-2} s^{-1}, 22°C/ 14-h dark at 18°C, 65% constant relative humidity). Cd tolerance index was quantified as EC_{100}, the effective Cd concentration causing 100% root growth inhibition (49). For transcriptome sequencing and multi-element analysis (Table S4), 1x modified Hoagland's solution was supplemented with either 2 or 0 (control) µM $CdSO_4$, with cultivation in 16-h light (90 µmol photons m^{-2} s^{-1}, 22°C)/ 8-h dark (18°C) cycles at 60% constant relative humidity for 16 d.

Multi-element analysis and transcriptome sequencing

For multi-element analysis, apoplastically bound metal cations were desorbed from freshly harvested roots (50). All tissues were washed twice in ddH_2O before drying, digestion and multi-element analysis as described (4). For transcriptome sequencing, root and shoot tissues were harvested separately 7 h after the onset of the light period, frozen immediately in liquid nitrogen, pooled from six replicate clones per genotype, treatment and experiment, and stored at -80°C. Total RNA was extracted from aliquots of tissue homogenates using the RNeasy Plant Mini Kit (Qiagen, Hilden, Germany). One µg of total RNA was used in NEBNext Ultra II RNA Library Prep Kit for Illumina (New England Biolabs, Frankfurt, Germany), followed by sequencing to obtain 14 to 29 mio. 150-bp read pairs per sample that passed quality filters (Novogene, Hongkong).

Data analysis

Reads were mapped to the *A. halleri* ssp. *gemmifera* (Matsumura) O'Kane & Al-Shehbaz accession Tada mine (W302) reference genome (51) using HISAT2 version 2.1.0 (52). After error correction according to COMEX 2.1 (53), the number of fragments per gene were determined using Qualimap2 (54), followed by principal component analysis (PCA) and differential gene expression analysis using the R package *DESeq2* (55). Clustering was performed using the R package *pheatmap*. For gene ontology (GO) term enrichment analyses *A. halleri* gene IDs were converted into *A. thaliana* TAIR10 AGI codes, which were then used in hypergeometric distribution estimation through the function g:GOSt built in g:Profiler (56). TE transcript levels were quantified based on Reads Per Kilobase per Million reads (57) after mapping to the *Arabidopsis lyrata* MN47 reference genome with TE annotations (53). Reads were used to reconstruct cDNA variants with Integrated Genome Viewer (58). Sequence data are available here (PRJEB35573, ENA, EMBL-EBI). Multiple comparisons of means were conducted using the *stats* and *agricolae*, with normality and homoscedasticity tests in the *car*, packages in R (59).

Validation by RT-qPCR and immunoblots

We used aliquots of homogenized tissues as frozen for transcriptome sequencing. Real-time RT-qPCR reactions were run in a 384-well LightCycler®480 II System (Roche Diagnostics, Mannheim, Germany) using the GoTaq qPCR Mastermix (Promega, Walldorf, Germany) and cDNAs synthesized from DNase-treated total RNA using the RevertAid First Strand cDNA Synthesis Kit (Thermo Fisher Scientific, Schwerte, Germany). Immunoblots were carried out following SDS-PAGE (60) using anti-*At*IRT1 (AS11 1780, Lot number 1203; Agrisera, Vännas, Sweden), anti-*At*ZYP1 (Raphael Mercier, Max Planck Institute for Plant Breeding Research, Cologne, Germany) and anti-*At*ACTIN (AS13

2640, Lot number 1711; Agrisera) primary antibodies, HRP-conjugated secondary antibodies (Thermo Fisher Scientific) and detection using the ECL Select Western Blotting Detection Reagent (GE Healthcare, Little Chalfont, England) and a Fusion Fx7 GelDoc (Vilber Lourmat, Eberhardzell, Germany).

Acknowledgements

We are grateful to Raphael Mercier (Max Planck Institute for Plant Breeding Research, Cologne, Germany) for materials. We thank Petra Düchting, Andreas Aufermann and Jan Riering for assistance (Ruhr University Bochum, Germany). This work was funded by the Research Priority Programs SPP1529 ADAPTOMICS (GL/JEA; Kr1967/10 and 12, UK) and SPP1819 RAPID EVOLUTION (Kr1967/16, UK), as well as grant Kr1967/3-3 (UK) of the Deutsche Forschungsgemeinschaft, and Ruhr University Bochum. We acknowledge the Bielefeld-Gießen Center for Microbial Bioinformatics (BiGi) of the BMBF-funded German network for bioinformatics infrastructure (de.NBI, grant 031A533) for providing computational resources and general support. Our research is supported by Advanced Grant LEAP-EXTREME (788380, UK) of the European Research Council.

References

1. Nriagu JO & Pacyna JM (1988) Quantitative assessment of worldwide contamination of air, water and soils by trace metals. *Nature* 333(6169):134-139.
2. Lamas GA, Navas-Acien A, Mark DB, & Lee KL (2016) Heavy Metals, Cardiovascular Disease, and the Unexpected Benefits of Chelation Therapy. *J Am Coll Cardiol* 67(20):2411-2418.
3. Ernst WHO (1974) *Schwermetallvegetationen der Erde* (Gustav Fischer Verlag, Stuttgart, Germany).
4. Stein RJ*, et al.* (2017) Relationships between soil and leaf mineral composition are element-specific, environment-dependent and geographically structured in the emerging model *Arabidopsis halleri*. *New Phytol* 213(3):1274-1286.
5. Reeves RD*, et al.* (2018) A global database for plants that hyperaccumulate metal and metalloid trace elements. *New Phytol* 218(2):407-411.
6. Kazemi-Dinan A, Thomaschky S, Stein RJ, Krämer U, & Müller C (2014) Zinc and cadmium hyperaccumulation act as deterrents towards specialist herbivores and impede the performance of a generalist herbivore. *New Phytol* 202(2):628-639.
7. Becher M, Talke IN, Krall L, & Krämer U (2004) Cross-species microarray transcript profiling reveals high constitutive expression of metal homeostasis genes in shoots of the zinc hyperaccumulator *Arabidopsis halleri*. *Plant J* 37(2):251-268.
8. Talke IN, Hanikenne M, & Krämer U (2006) Zinc-Dependent Global Transcriptional Control, Transcriptional Deregulation, and Higher Gene Copy Number for Genes in Metal Homeostasis of the Hyperaccumulator *Arabidopsis halleri*. *Plant Physiol* 142(1):148-167.
9. Weber M, Harada E, Vess C, Roepenack-Lahaye EV, & Clemens S (2004) Comparative microarray analysis of *Arabidopsis thaliana* and *Arabidopsis halleri* roots identifies nicotianamine synthase, a ZIP transporter and other genes as potential metal hyperaccumulation factors. *Plant J* 37:269-281.

10. Hanikenne M*, et al.* (2008) Evolution of metal hyperaccumulation required *cis*-regulatory changes and triplication of *HMA4*. *Nature* 453:391-395.
11. Deinlein U*, et al.* (2012) Elevated nicotianamine levels in *Arabidopsis halleri* roots play a key role in zinc hyperaccumulation. *Plant Cell* 24(2):708-723.
12. Dräger DB*, et al.* (2004) Two genes encoding *Arabidopsis halleri* MTP1 METAL TRANSPORT PROTEINS co-segregate with zinc tolerance and account for high *MTP1* transcript levels. *Plant J* 39(3):425-439.
13. Baliardini C, Meyer CL, Salis P, Saumitou-Laprade P, & Verbruggen N (2015) CATION EXCHANGER1 cosegregates with cadmium tolerance in the metal hyperaccumulator *Arabidopsis halleri* and plays a role in limiting oxidative stress in *Arabidopsis* spp. *Plant Physiol* 169(1):549-559.
14. Meyer CL*, et al.* (2015) Intraspecific variability of cadmium tolerance and accumulation, and cadmium-induced cell wall modifications in the metal hyperaccumulator *Arabidopsis halleri*. *J Exp Bot* 66(11):3215-3227.
15. Corso M*, et al.* (2018) Contrasting cadmium resistance strategies in two metallicolous populations of Arabidopsis halleri. *New Phytol* 218(1):283-297.
16. Schvartzman MS*, et al.* (2018) Adaptation to high zinc depends on distinct mechanisms in metallicolous populations of *Arabidopsis halleri*. *New Phytol* 218(1):269-282.
17. Duran-Figueroa N & Vielle-Calzada JP (2010) ARGONAUTE9-dependent silencing of transposable elements in pericentromeric regions of Arabidopsis. *Plant Signal Behav* 5(11):1476-1479.
18. Olmedo-Monfil V*, et al.* (2010) Control of female gamete formation by a small RNA pathway in Arabidopsis. *Nature* 464(7288):628-632.
19. Vaucheret H (2008) Plant ARGONAUTES. *Trends Plant Sci* 13(7):350-358.
20. Vert G*, et al.* (2002) IRT1, an Arabidopsis transporter essential for iron uptake from the soil and for plant growth. *Plant Cell* 14(6):1223-1233.
21. Kerkeb L*, et al.* (2008) Iron-induced turnover of the Arabidopsis IRON-REGULATED TRANSPORTER1 metal transporter requires lysine residues. *Plant Physiol* 146(4):1964-1973.
22. Callis J (2014) The ubiquitination machinery of the ubiquitin system. *Arabidopsis Book* 12:e0174.
23. Barberon M*, et al.* (2011) Monoubiquitin-dependent endocytosis of the IRON-REGULATED TRANSPORTER 1 (IRT1) controls iron uptake in plants. *Proc Natl Acad Sci USA* 108(32):E450-458.
24. Weber M, Trampczynska A, & Clemens S (2006) Comparative transcriptome analysis of toxic metal responses in *Arabidopsis thaliana* and the Cd^{2+}-hypertolerant facultative metallophyte *Arabidopsis halleri*. *Plant Cell Environ* 29(5):950-963.
25. Mercier R, Mezard C, Jenczewski E, Macaisne N, & Grelon M (2015) The molecular biology of meiosis in plants. *Annu Rev Plant Biol* 66:297-327.
26. Schuermann D, Molinier J, Fritsch O, & Hohn B (2005) The dual nature of homologous recombination in plants. *Trends Genet* 21(3):172-181.
27. Rounds MA & Larsen PB (2008) Aluminum-dependent root-growth inhibition in Arabidopsis results from AtATR-regulated cell-cycle arrest. *Curr Biol* 18(19):1495-1500.
28. Kovalchuk O, Titov V, Hohn B, & Kovalchuk I (2001) A sensitive transgenic plant system to detect toxic inorganic compounds in the environment. *Nat Biotechnol* 19(6):568-572.
29. Morales ME*, et al.* (2016) Heavy Metal Exposure Influences Double Strand Break DNA Repair Outcomes. *PLoS One* 11(3):e0151367.
30. Sakamoto T*, et al.* (2011) Condensin II alleviates DNA damage and is essential for tolerance of boron overload stress in Arabidopsis. *Plant Cell* 23(9):3533-3546.
31. Seeliger K, Dukowic-Schulze S, Wurz-Wildersinn R, Pacher M, & Puchta H (2012) BRCA2 is a mediator of RAD51- and DMC1-facilitated homologous recombination in *Arabidopsis thaliana*. *New Phytol* 193(2):364-375.
32. Geuting V*, et al.* (2009) Two distinct MUS81-EME1 complexes from Arabidopsis process Holliday junctions. *Plant Physiol* 150(2):1062-1071.
33. Bouyer D*, et al.* (2018) Genome-wide identification of RETINOBLASTOMA RELATED 1 binding sites in Arabidopsis reveals novel DNA damage regulators. *PLoS Genet* 14(11):e1007797.

34. Fernandes JB*, et al.* (2018) FIGL1 and its novel partner FLIP form a conserved complex that regulates homologous recombination. *PLoS Genet* 14(4):e1007317.
35. Liu M*, et al.* (2017) IDN2 Interacts with RPA and Facilitates DNA Double-Strand Break Repair by Homologous Recombination in Arabidopsis. *Plant Cell* 29(3):589-599.
36. Dubest S, Gallego ME, & White CI (2004) Roles of the AtERCC1 protein in recombination. *Plant J* 39(3):334-342.
37. Hefner E, Preuss SB, & Britt AB (2003) Arabidopsis mutants sensitive to gamma radiation include the homologue of the human repair gene ERCC1. *J Exp Bot* 54(383):669-680.
38. Grandbastien MA (2015) LTR retrotransposons, handy hitchhikers of plant regulation and stress response. *Biochim Biophys Acta* 1849(4):403-416.
39. Horvath V, Merenciano M, & Gonzalez J (2017) Revisiting the Relationship between Transposable Elements and the Eukaryotic Stress Response. *Trends Genet* 33(11):832-841.
40. Krämer U (2018) Conceptualizing plant systems evolution. *Curr Opin Plant Biol* 42:66-75.
41. Oliver C, Santos JL, & Pradillo M (2014) On the role of some ARGONAUTE proteins in meiosis and DNA repair in *Arabidopsis thaliana*. *Front Plant Sci* 5:177.
42. Higgins JD, Sanchez-Moran E, Armstrong SJ, Jones GH, & Franklin FC (2005) The Arabidopsis synaptonemal complex protein ZYP1 is required for chromosome synapsis and normal fidelity of crossing over. *Genes Dev* 19(20):2488-2500.
43. Osman K, Sanchez-Moran E, Higgins JD, Jones GH, & Franklin FC (2006) Chromosome synapsis in Arabidopsis: analysis of the transverse filament protein ZYP1 reveals novel functions for the synaptonemal complex. *Chromosoma* 115(3):212-219.
44. Spampinato CP (2017) Protecting DNA from errors and damage: an overview of DNA repair mechanisms in plants compared to mammals. *Cell Mol Life Sci* 74(9):1693-1709.
45. Hussain D*, et al.* (2004) P-type ATPase heavy metal transporters with roles in essential zinc homeostasis in Arabidopsis. *Plant Cell* 16(5):1327-1339.
46. Sinclair SA*, et al.* (2018) Systemic Upregulation of MTP2- and HMA2-Mediated Zn Partitioning to the Shoot Supplements Local Zn Deficiency Responses. *Plant Cell* 30(10):2463-2479.
47. Leskova A, Giehl RFH, Hartmann A, Fargasova A, & von Wiren N (2017) Heavy Metals Induce Iron Deficiency Responses at Different Hierarchic and Regulatory Levels. *Plant Physiol* 174(3):1648-1668.
48. Halimaa P*, et al.* (2019) Transcriptional effects of cadmium on iron homeostasis differ in calamine accessions of *Noccaea caerulescens*. *Plant J* 97(2):306-320.
49. Schat H & Ten Bookum WM (1992) Genetic control of copper tolerance in *Silene vulgaris*. *Heredity* 68(3):219-229.
50. Cailliatte R, Schikora A, Briat JF, Mari S, & Curie C (2010) High-affinity manganese uptake by the metal transporter NRAMP1 is essential for Arabidopsis growth in low manganese conditions. *Plant Cell* 22(3):904-917.
51. Briskine RV*, et al.* (2017) Genome assembly and annotation of *Arabidopsis halleri*, a model for heavy metal hyperaccumulation and evolutionary ecology. *Mol Ecol Resour* 17(5):1025-1036.
52. Kim D, Langmead B, & Salzberg SL (2015) HISAT: a fast spliced aligner with low memory requirements. *Nat Methods* 12(4):357-360.
53. Pietzenuk B*, et al.* (2016) Recurrent evolution of heat-responsiveness in Brassicaceae COPIA elements. *Genome Biol* 17(1):209.
54. Okonechnikov K, Conesa A, & Garcia-Alcalde F (2016) Qualimap 2: advanced multi-sample quality control for high-throughput sequencing data. *Bioinformatics* 32(2):292-294.
55. Love MI, Huber W, & Anders S (2014) Moderated estimation of fold change and dispersion for RNA-seq data with DESeq2. *Genome Biol* 15(12):550.
56. Reimand J*, et al.* (2016) g:Profiler-a web server for functional interpretation of gene lists (2016 update). *Nucleic Acids Res* 44(W1):W83-89.
57. Mortazavi A, Williams BA, McCue K, Schaeffer L, & Wold B (2008) Mapping and quantifying mammalian transcriptomes by RNA-Seq. *Nat Methods* 5(7):621-628.

58. Robinson JT, Thorvaldsdottir H, Wenger AM, Zehir A, & Mesirov JP (2017) Variant Review with the Integrative Genomics Viewer. *Cancer Res* 77(21):e31-e34.
59. R_Core_Team (2013) R: A language and environment for statistical computing. (Foundation for Statistical Computing, Vienna, Austria).
60. Lämmli UK (1970) Cleavage of structural proteins during the assembly of the head of bacteriophage T4. *Nature* 227(5259):680-685.

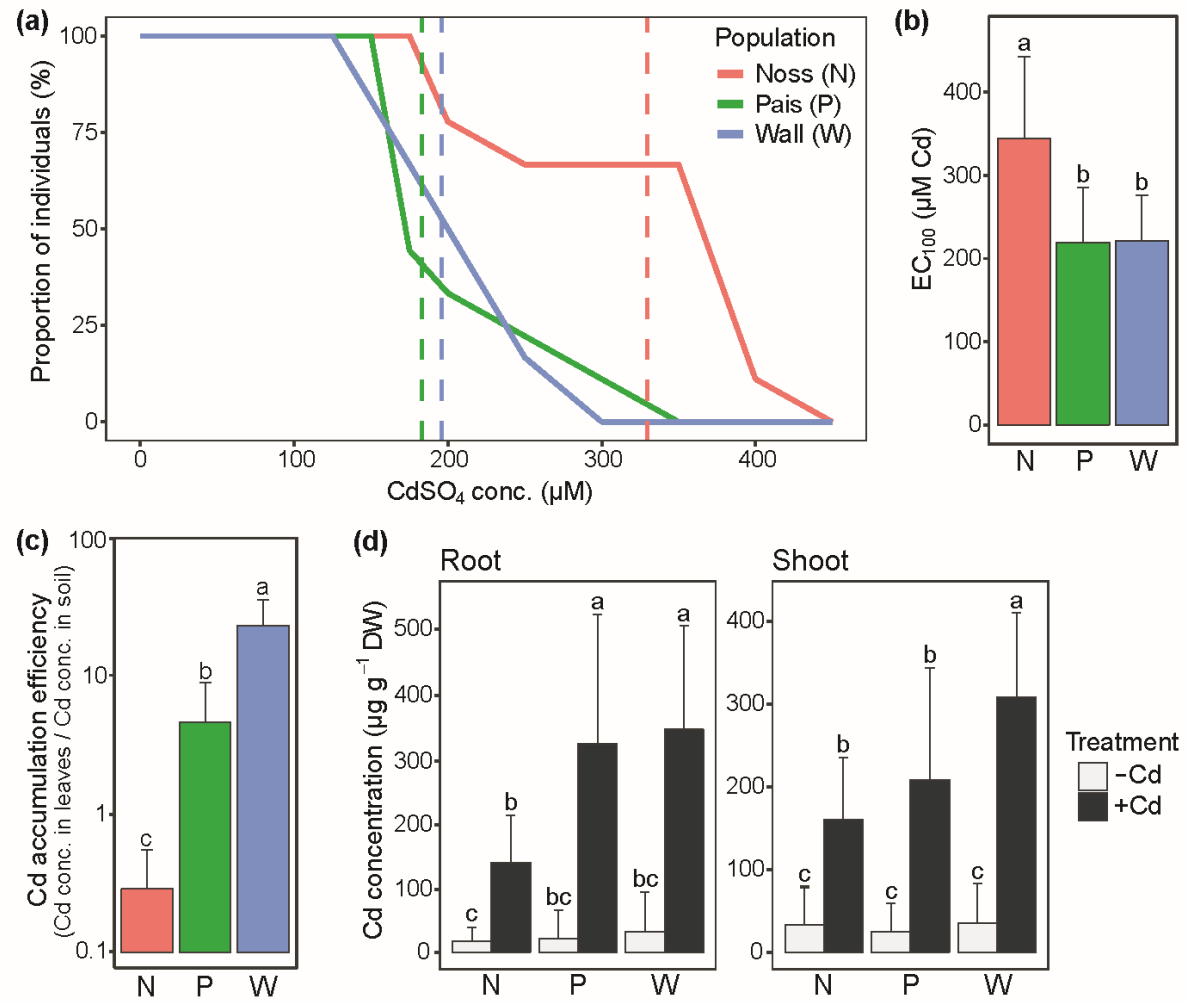

Fig. 1 Cadmium tolerance and accumulation in three populations of *A. halleri*. (a) Proportion of individuals maintaining root growth (elongation) as a function of Cd concentration. Dashed vertical lines indicate ED_{50} (i.e., the effective dose required to reach a proportion of 50% according to a dose-response model; see Table S2). (b) Effective Cd concentration causing 100% root growth inhibition (EC_{100}; bars represent mean ± SD). Plants were sequentially exposed to stepwise increasing concentrations of $CdSO_4$ in hydroponic culture every week (*n* = 6 to 9 per population, with one to three vegetative clones of each three to six genotypes per population; (a, b)). (c) Cd accumulation efficiency at the site of origin calculated from published field survey data (bars represent means ± SD of *n* = 11 to 12 individuals in the field; units employed, μg Cd g^{-1} dry biomass in leaves, μg total Cd g^{-1} dry mass in soil; data from Stein *et al.*, 2017). (d) Cd concentration in root and shoot tissues of hydroponically cultivated plants. Shown are mean ± SD (*n* = 12 to 20 clones per population comprising both genotypes, from all three replicate experiments; see Table S1). Four-week-old vegetative clones were exposed to 0 (-Cd) and 2 μM $CdSO_4$ (+Cd) in hydroponic culture for 16 d alongside the plants cultivated for RNA-seq. Different characters denote statistically significant differences between means based on two-way ANOVA, followed by Tukey's HSD test (Log-transformed data were used in (c)) ($P < 0.05$; see Table S3 for nested ANOVA of genotypes within a population (d)).

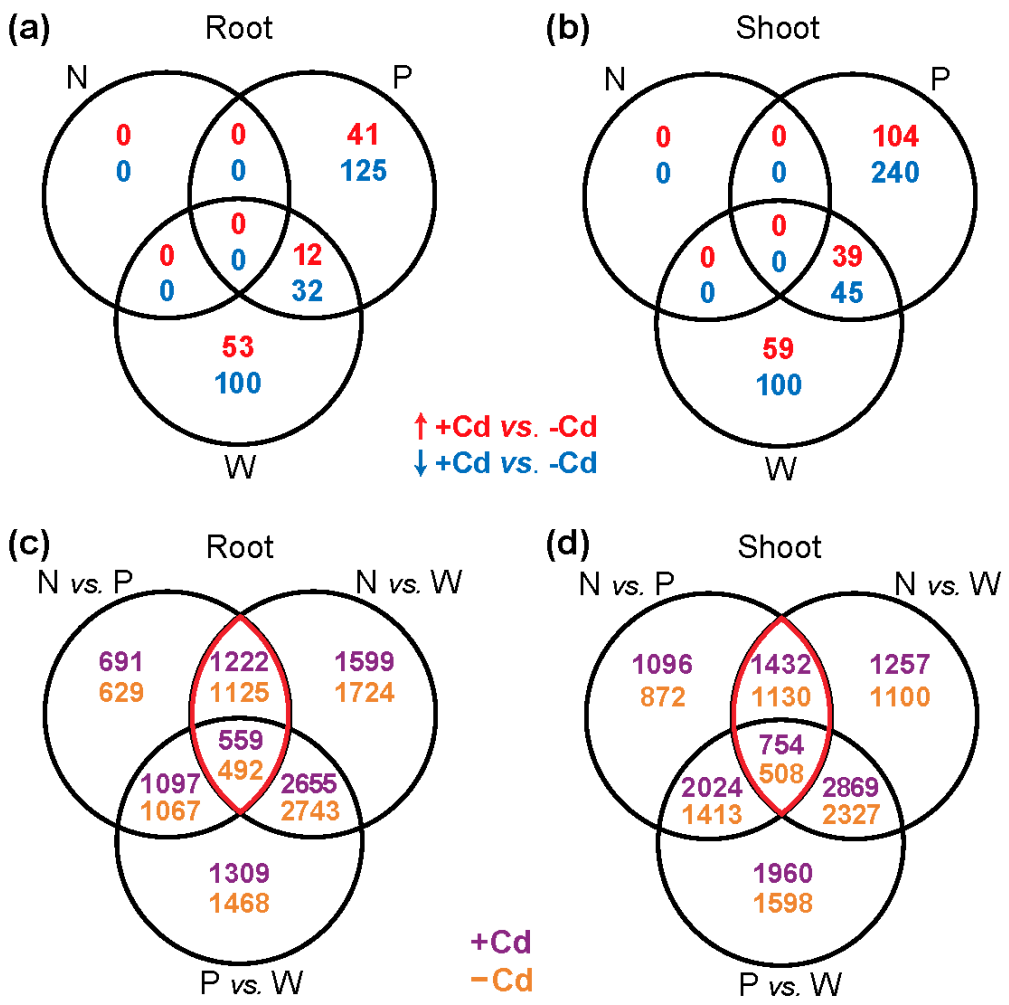

Fig. 2 Between-population differences according to transcriptome sequencing. (a, b) Venn diagrams show the numbers of genes exhibiting differential transcript abundances under exposure to Cd (+Cd) compared to control conditions (-Cd) for the three populations Noss (N), Pais (P) and Wall (W) in root (a) and shoot (b) tissues. Upregulation (red): Log_2(fold change +Cd *vs.* –Cd) = $Log_2FC > 0.5$; downregulation (blue): $Log_2FC < -0.5$; all with adjusted *P*-value < 0.05. (c, d) Venn diagrams show the numbers of genes exhibiting differential transcript abundance between populations in root (c) and shoot (d) tissues of plants cultivated under Cd exposure (violet) or control conditions (orange) ($|Log_2FC| > 0.5$; adjusted *P*-value < 0.05). Red lines surround genes differentially expressed between Noss and both populations of NM soils (Pais and Wall). Four-week-old vegetative clones were exposed to 2 µM Cd or 0 µM Cd (controls) in hydroponic culture for 16 d before harvest. Data are from three independent experiments (repeats), with two genotypes per population and material pooled from six replicate vegetative clones (three hydroponic culture vessels) per genotype in each experiment.

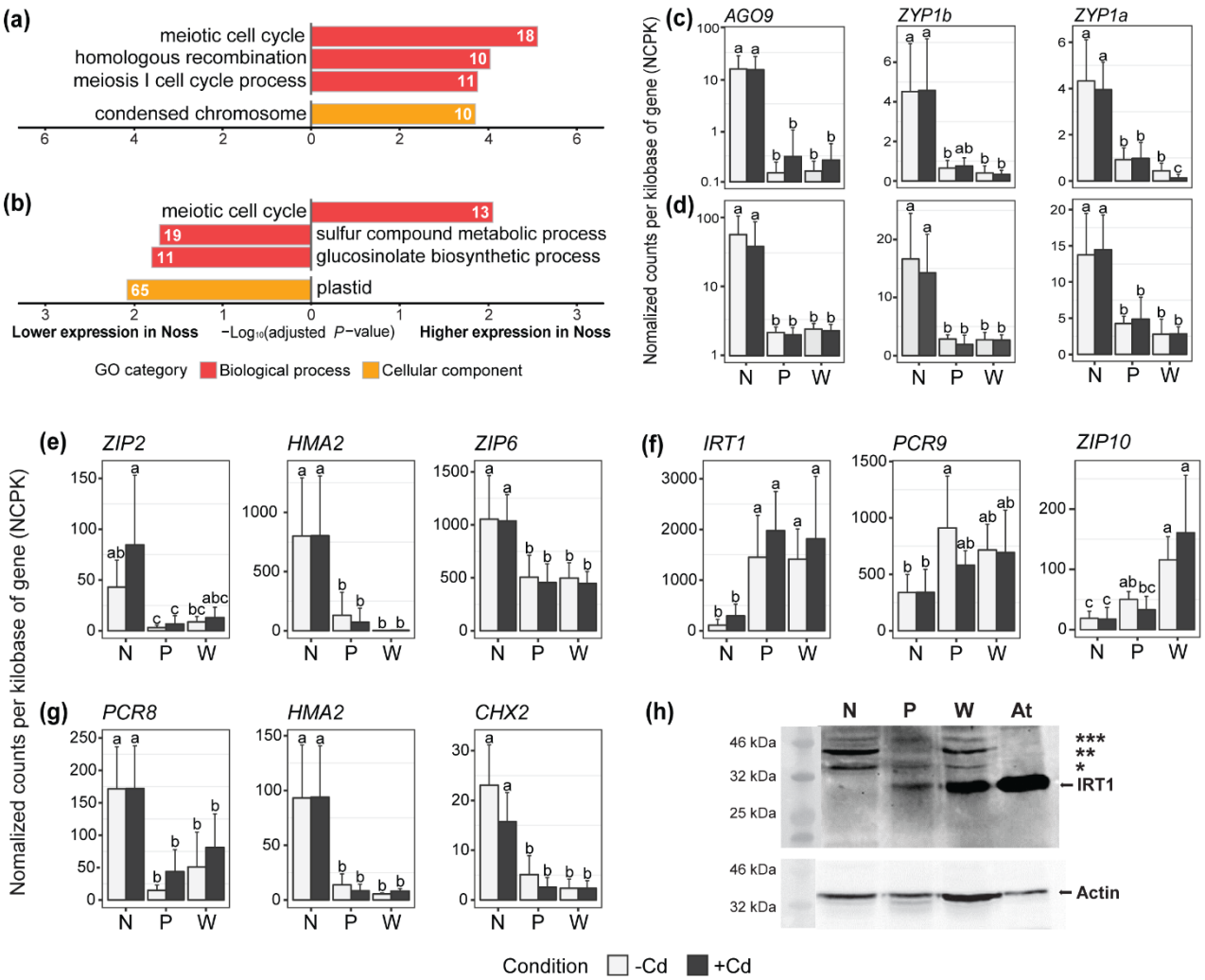

Fig. 3 Candidate genes differentially expressed in Noss compared to both other populations Pais and Wall. (a, b) Significantly enriched gene ontology (GO) categories for roots (a) and shoots (b) of plants cultivated in 0 µM Cd (adjusted *P*-value < 0.05). Genes differentially expressed between Noss from M soil and both Pais and Wall from NM soils were subjected to a GO term enrichment analysis. The number of genes in each over-represented category is shown inside bars (see Dataset S4 for all genes). (c, d) Relative transcript levels of the top three genes (largest between-population differences) taken from (a) and (b) in the over-represented GO category meiotic cell cycle, for roots (c) and shoots (d). (e-g) Relative transcript levels of metal homeostasis genes of which transcript levels are high (e, g) and low (f) in Noss (N) compared to both Pais (P) and Wall (W), for roots (e, f) and shoots (g) (top three genes from Table S8). Bars show means ± SD (*n* = 6) of normalized counts, which were additionally normalized per kilobase of gene length (NCPK). Different characters represent statistically significant groups based on two-way ANOVA, followed by Tukey's HSD test (*P* < 0.05, see Table S6 for details). Data are from the same experiment as shown in Fig. 2. (h) Immunoblot detection of IRT1. Total protein extracts (40 µg) from roots of Noss_05 (N), Pais_09 (P) and Wall_07 (W) cultivated under control condition as used in transcriptome sequencing, and total protein extract (10 µg) from roots of Fe- and Zn-deficient *A. thaliana* (*At*; positive control) were separated on a denaturing polyacrylamide gel, blotted, and detection was carried out using an anti-IRT1 or an anti-actin antibody. Asterisks mark additional bands at positions consistent with *IRT1-Ub (mono-ubiquitinated form), **IRT1-Ub_2, *** IRT1-Ub_3, respectively.

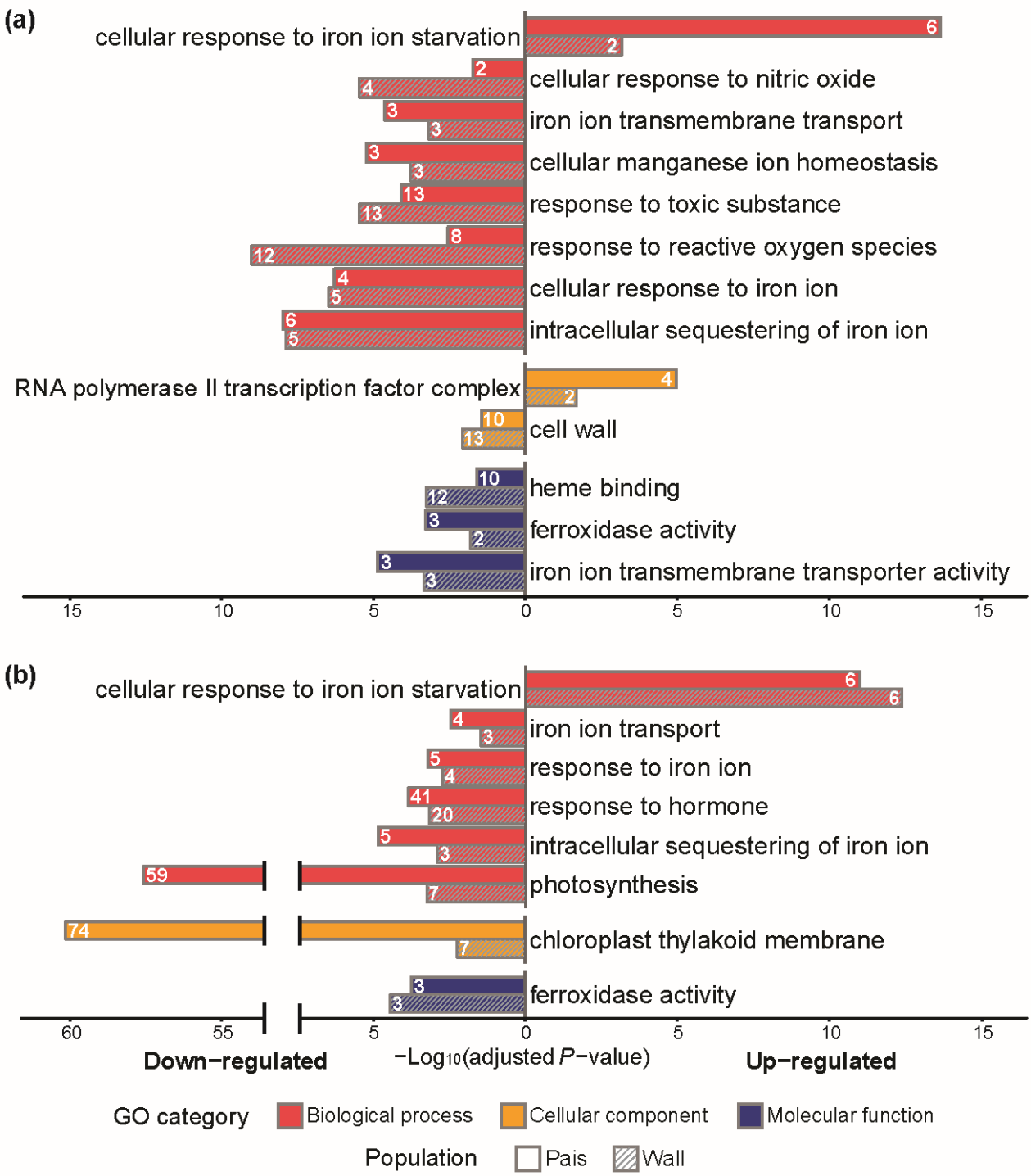

Fig. 4 Functional classification of the transcriptional response to Cd. Significantly enriched GO categories among the transcriptional responses to Cd common in both the Pais and Wall populations for roots (a) and shoots (b) (see Fig. 2a, b; Dataset S6). The numbers of genes in each over-represented category are shown inside bars. Data are from the same experiment as shown in Fig. 2.

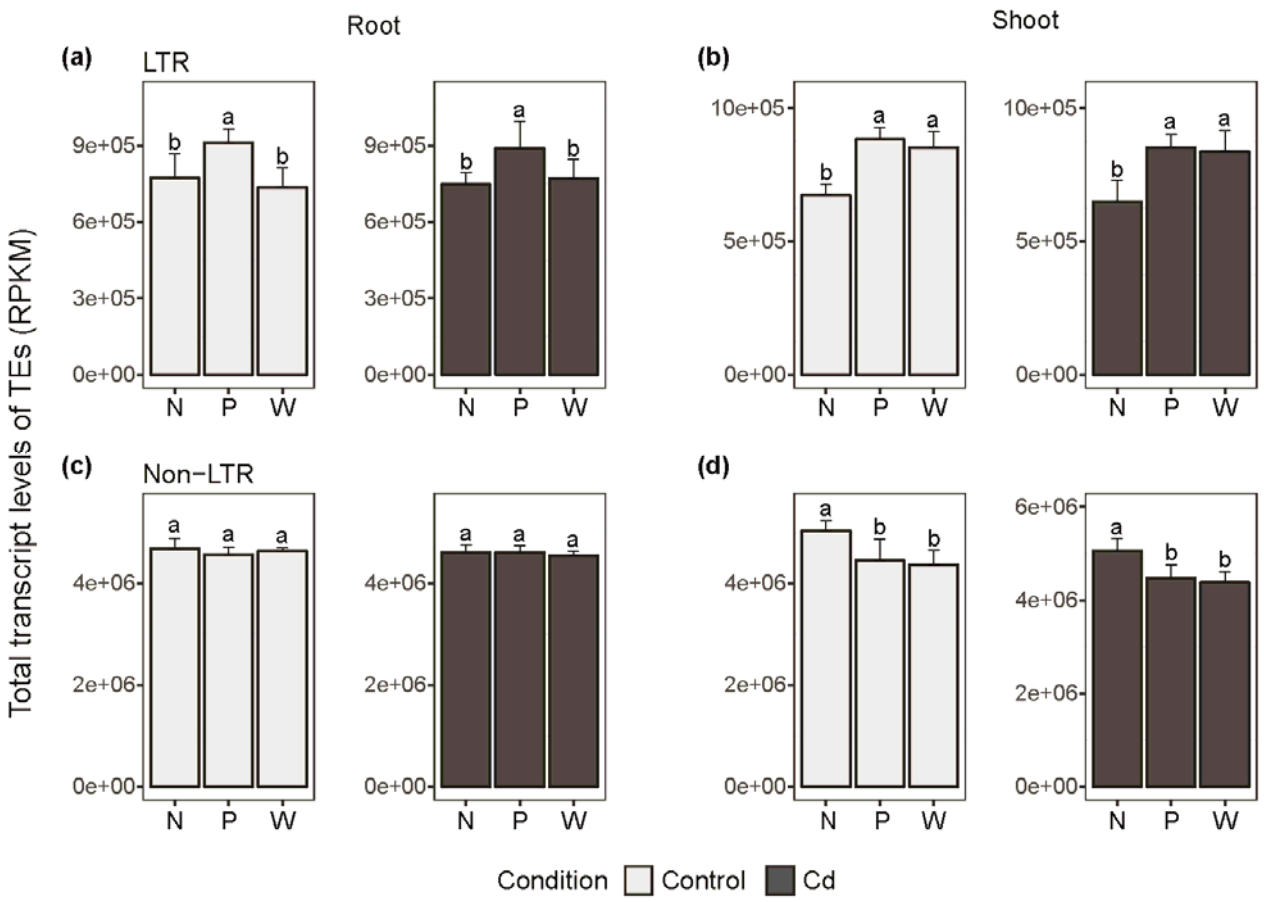

Fig. 5 Genome-wide sum of transcript levels contributed by different types of transposable elements in Noss, Pais and Wall. (a-d) Bars show means ± SD (n = 6) of transcript levels of transposable elements (TEs), corresponding to the sum total of RPKM for LTR (Long terminal repeat) retrotransposons (a, b) and non-LTR TEs (c, d) in root (a, c) and shoot (b, d), with RPKM $\geq$ 7 per locus. Different characters represent statistically significant differences based on one-way ANOVA, followed by Tukey's HSD test ($P < 0.05$).